

# Measuring the one-particle excitations of ultracold fermionic atoms by stimulated Raman spectroscopy

Tung-Lam Dao,<sup>1</sup> Antoine Georges,<sup>1</sup> Jean Dalibard,<sup>2</sup> Christophe Salomon,<sup>2</sup> and Iacopo Carusotto<sup>3</sup>

<sup>1</sup>*Centre de Physique Théorique, CNRS UMR 7644, Ecole Polytechnique, Route de Saclay, 91128 Palaiseau Cedex, France*

<sup>2</sup>*Laboratoire Kastler-Brossel, Ecole Normale Supérieure, 24, rue Lhomond, 75231 Paris Cedex 05, France*

<sup>3</sup>*CNR-INFM BEC Center and università di Trento, 38050 Povo, Italy*

(Dated: November 6, 2006)

We propose a Raman spectroscopy technique which is able to probe the one-particle Green's function, the Fermi surface, and the quasiparticles of a gas of strongly interacting ultracold atoms. We give quantitative examples of experimentally accessible spectra. The efficiency of the method is validated by means of simulated images for the case of a usual Fermi liquid as well as for more exotic states: specific signatures of e.g. a d-wave pseudo-gap are clearly visible.

PACS numbers: 03.75.Lm, 32.80.Pj, 71.30.+h, 71.10.Fd

The remarkable advances in handling ultra-cold atomic gases have given birth to the new field of “condensed matter physics with light and atoms”. Key issues in the physics of strongly correlated quantum systems can be addressed from a new perspective in this context. The observation of the Mott transition of bosons in optical lattices [1] and of the superfluidity of fermionic gases [2] have been important milestones in this respect, as well as the recent imaging of Fermi surfaces [3]. Ultimately fermionic atoms in optical lattices (see [4] for a review) could help understanding some outstanding problems of condensed matter physics, such as high-temperature superconductivity. In this context, a key issue is the nature of the low-energy excitations of low-dimensional strongly interacting Fermi systems. There is abundant experimental evidence that those are highly unconventional, departing from standard Fermi-liquid theory. In this Letter, we study how stimulated Raman spectroscopy can be used in order to probe the one-particle excitations of interacting ultracold fermionic atoms. We demonstrate the possibility of measuring the Fermi surface, of probing some of the quasiparticle properties and of revealing unconventional phenomena such as the pseudogap.

In a conventional Fermi liquid, low-energy excitations are built out of quasiparticles [5]. Those are characterized by their dispersion relation, i.e the energy  $\xi_{\mathbf{k}}$  (measured from the ground-state energy) necessary to create such an excitation with (quasi-) momentum  $\mathbf{k}$ . The interacting system possesses a Fermi surface (FS) defined by the location in momentum space on which the excitation energy vanishes:  $\xi_{\mathbf{k}_F} = 0$ . Close to a given point on the FS, the quasiparticle energy vanishes as:  $\xi_{\mathbf{k}} \sim \mathbf{v}_F(\mathbf{k}_F) \cdot (\mathbf{k} - \mathbf{k}_F) + \dots$ , with  $\mathbf{v}_F$  the local Fermi velocity (inversely related to the effective mass). Quasiparticle excitations have a finite lifetime  $\Gamma_{\mathbf{k}}^{-1}$ , and are well defined provided  $\Gamma_{\mathbf{k}}$  vanishes faster than  $\xi_{\mathbf{k}}$  as the FS is approached ( $\Gamma_{\mathbf{k}} \sim \xi_{\mathbf{k}}^2$  in Fermi liquid theory). In contrast, one-particle excitations in the “nor-

mal” (i.e non-superconducting) state of the cuprate superconductors (SC) reveal strong deviations from this behaviour [6]. Reasonably well-defined quasiparticle excitations only exist close to the diagonal direction of the Brillouin zone (the “nodal” direction along which the d-wave gap vanishes in the SC phase), and even there  $\Gamma_{\mathbf{k}}$  is rather large. Away from this direction (in the “antinodal” region), excitations appear to be short-lived and gapped already above the SC critical temperature (the so-called pseudogap phenomenon). This momentum-space differentiation is a key to the physics of cuprates. In fact, recent theoretical investigations [7] by a variety of methods strongly suggest that this phenomenon is present in simple theoretical models such as the two-dimensional Hubbard model.

Experiments probing directly non-diagonal one-particle correlators  $\langle \psi^\dagger(\mathbf{r}, t) \psi(\mathbf{r}', t') \rangle$  of a many-body system are therefore highly desirable but also relatively scarce. Most physical measurements indeed provide information on two-particle correlators of the form  $\langle \psi(\mathbf{r}, t)^\dagger \psi(\mathbf{r}, t) \psi^\dagger(\mathbf{r}', t') \psi(\mathbf{r}', t') \rangle$  [24]. Examples are neutron scattering or transport measurements in the solid-state context [8], and Bragg scattering [9] or noise correlations measurements [10] in the cold atom context. For Bose systems with a finite condensate density  $n_0$ , the two-particle correlator is closely related to the one-particle correlator via terms such as  $n_0 \langle \psi^\dagger(\mathbf{r}, t) \psi(\mathbf{r}', t') \rangle$ . By contrast, in Fermi systems the distinction between one- and two-particle correlators is essential.

In solids, angle-resolved photoemission spectroscopy (ARPES) provides a direct probe of the one-particle spectrum [11], and has played a key role in revealing momentum-space differentiation in cuprates [6]. It consists in measuring the energy and momentum of electrons emitted out of the solid exposed to an incident photon beam. In the simplest approximation, the emitted intensity can be related to the single-electron spectral function, defined at  $T = 0$  and for  $\omega < 0$ , i.e for

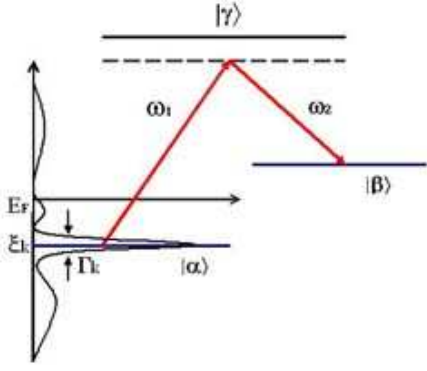


FIG. 1: Raman process: transfer from an internal state  $\alpha$  to another internal state  $\beta$  through an excited state  $\gamma$ . The momentum-resolved spectral function is schematized, consisting of a quasiparticle peak and an incoherent background.

hole-like excitations or electron removal by:  $A(\mathbf{k}, \omega) = \sum_n |\langle \Psi_n^{N-1} | \psi_{\mathbf{k}} | \Psi_0^N \rangle|^2 \delta(\omega + \mu + E_n - E_0)$ . In this expression,  $\psi_{\mathbf{k}}$  is a destruction operator for a particle with momentum  $\mathbf{k}$ ,  $\Psi_0^N$  is the ground-state of the  $N$ -particle system and  $\Psi_n^{N-1}$  are the eigenstates of the system with one less particle. In a conventional Fermi liquid, and for momenta close to the FS, the spectral function can be separated into a coherent quasiparticle contribution and an incoherent contribution (Fig. 1):  $A = A_{\text{QP}} + A_{\text{inc}}$ , with  $A_{\text{QP}}(\mathbf{k}, \omega) \simeq Z_{\mathbf{k}} \frac{\Gamma_{\mathbf{k}}}{\pi[(\omega - \xi_{\mathbf{k}})^2 + \Gamma_{\mathbf{k}}^2]}$  and  $A_{\text{inc}}$  widely spread in frequency. Only a finite fraction  $Z_{\mathbf{k}} < 1$  of the total spectral weight corresponds to long-lived quasiparticle excitations.

In this paper, we consider stimulated Raman spectroscopy as a probe of one-particle excitations in a two-component mixture of ultracold fermionic atoms in two internal states  $\alpha$  and  $\alpha'$ . Stimulated Raman spectroscopy has been considered previously in the context of cold atomic gases, both as an outcoupling technique to produce an atom laser [12] and as a measurement technique for bosons [13–16] and fermions [17, 18]. In the Raman process of Fig. 1, atoms are transferred from  $\alpha$  into another internal state  $\beta \neq \alpha, \alpha'$ , through an intermediate excited state  $\gamma$ , using two laser beams of wavevectors  $\mathbf{k}_{1,2}$  and frequencies  $\omega_{1,2}$ . If  $\omega_1$  is sufficiently far from single photon resonance to the excited  $\gamma$  state, we can neglect spontaneous emission. Eliminating the excited state, we write an effective hamiltonian:  $\hat{V} = C \int d\mathbf{r} \psi_{\alpha}^{\dagger}(\mathbf{r}) \psi_{\beta}(\mathbf{r}) e^{i(\mathbf{k}_1 - \mathbf{k}_2) \cdot \mathbf{r}} a_1^{\dagger} a_2 + \text{h.c.}$ , in which  $a_1^{\dagger}$  ( $a_2$ ) denotes the creation (destruction) operator of a photon respectively in mode 1 (2) and the constant  $C$  is proportional to the product of the dipole matrix elements  $d_{\alpha\gamma}$  and  $d_{\beta\gamma}$  of the optical transitions and inversely proportional to the detuning from the excited state.

The total transfer rate to state  $\beta$  can be calculated [13–

15] using the Fermi golden rule:

$$R(\mathbf{q}, \Omega) = |C|^2 n_1 (n_2 + 1) \int_{-\infty}^{\infty} dt \int d\mathbf{r} d\mathbf{r}' e^{i[\Omega t - \mathbf{q} \cdot (\mathbf{r} - \mathbf{r}')] } \times g_{\beta}(\mathbf{r}, \mathbf{r}'; t) \langle \psi_{\alpha}^{\dagger}(\mathbf{r}, t) \psi_{\alpha}(\mathbf{r}', 0) \rangle. \quad (1)$$

Here  $\mathbf{q} = \mathbf{k}_1 - \mathbf{k}_2$  and  $\Omega = \omega_1 - \omega_2 + \mu$  with  $\mu$  the chemical potential of the interacting gas, and  $n_{1,2}$  the photon numbers present in the laser beams. Assuming that no atoms are initially present in  $\beta$  and that the scattered atoms in  $\beta$  do not interact with the atoms in the initial  $\alpha, \alpha'$  states, the free propagator for  $\beta$ -state atoms in vacuum is to be taken:  $g_{\beta}(\mathbf{r}, \mathbf{r}'; t) \equiv \langle 0_{\beta} | \psi_{\beta}(\mathbf{r}, t) \psi_{\beta}^{\dagger}(\mathbf{r}', 0) | 0_{\beta} \rangle$ . The correlation function entering (1) is proportional to the one-particle Green's function [25]  $\langle \psi_{\alpha}^{\dagger}(\mathbf{r}, t) \psi_{\alpha}(\mathbf{r}', 0) \rangle = -iG_{\alpha}^{<}(\mathbf{r}', \mathbf{r}, -t)$  of the (possibly strongly interacting) Fermi system. For a uniform system, the rate (1) can be related to the spectral function  $A(\mathbf{k}, \omega)$  of atoms in the internal state  $\alpha$  by [14]:

$$R(\mathbf{q}, \Omega) \propto \int d\mathbf{k} n_F(\varepsilon_{\mathbf{k}\beta} - \Omega) A(\mathbf{k} - \mathbf{q}, \varepsilon_{\mathbf{k}\beta} - \Omega) \quad (2)$$

in which the Green's function has been expressed in terms of the spectral function and the Fermi factor  $n_F$  as [8]:  $G_{\alpha}^{<}(\mathbf{k}, \omega) = i n_F(\omega) A(\mathbf{k}, \omega)$ .

In order to physically understand which information can be extracted from a measurement of the rate (2), let us consider first the simplest case of a non-interacting gas at  $T = 0$ . Then,  $n_F(\omega) = \Theta(-\omega)$  and  $A(\mathbf{k}, \omega) = \delta(\omega - \xi_{\mathbf{k}}^0)$  with  $\xi_{\mathbf{k}}^0 = \varepsilon_{\mathbf{k}\alpha} - \mu$  the single-particle energies for the  $\alpha$  state (counted from the Fermi energy). The Raman rate then reads:  $R = \int_{\xi_{\mathbf{k}}^0 < 0} d\mathbf{k} \delta(\varepsilon_{\mathbf{k}+\mathbf{q},\beta} - \xi_{\mathbf{k}}^0 - \Omega)$ . Contributions to this integral come from momenta inside the FS ( $\xi_{\mathbf{k}}^0 < 0$ ) which satisfy the Raman resonance condition  $\varepsilon_{\mathbf{k}+\mathbf{q},\beta} - \xi_{\mathbf{k}}^0 = \Omega$ . When the frequency shift  $\Omega$  is too small,  $R$  vanishes since there is no available phase-space satisfying these constraints. The smallest frequency at which a signal starts to be observed is  $\Omega_T = \text{Min}_{\mathbf{k}} \varepsilon_{\mathbf{k}\beta} \equiv \varepsilon_{\beta}^0$ , corresponding to a momentum transfer  $\mathbf{q} = -\mathbf{k}_F$  which lies itself on the FS [26]. This provides a simple way of determining the FS: by tuning  $\Omega$  very close to the extinction threshold  $\Delta\Omega = \Omega - \Omega_T \gtrsim 0$  and sweeping over the momentum transfer  $\mathbf{q}$ , the region in momentum space inside which a sizeable transfer rate  $R$  is measured consists of a shell surrounding the FS, with a finite width (measured parallel to the local Fermi velocity)  $\Delta\mathbf{q}_{\parallel} \sim \sqrt{2M \Delta\Omega}$ . In this expression  $M$  is the effective mass at the bottom of the  $\beta$ -band.

This analysis extends to the case of a Fermi liquid with well-defined quasiparticles near the FS, whose spectral function has a Lorentzian form with an inverse lifetime  $\Gamma$ . The width of the momentum-space shell then reads  $\Delta\mathbf{q}_{\parallel} \sim \sqrt{2M \Delta\Omega} + \Gamma/v_F$ , so that a study of the Raman signal near threshold provides information not only on the shape of the FS but also on the lifetime of the quasiparticles.

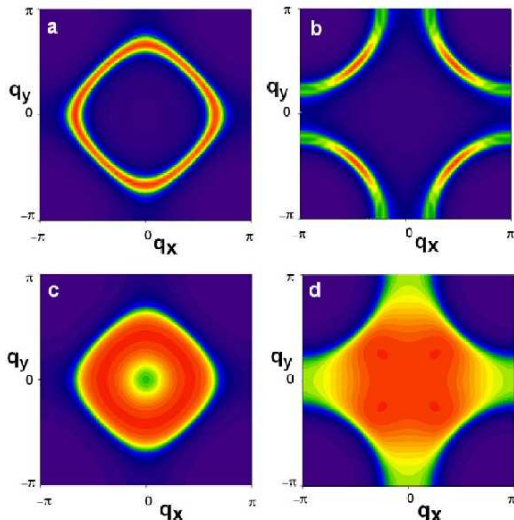


FIG. 2: Intensity plots of the Raman rate  $R(\mathbf{q}, \Omega)$ , for  $\Omega$  close to threshold  $\Omega_T$  ( $\Delta\Omega = 0.01t_\alpha$ ). (a) Non-interacting fermions on the homogeneous 2D square lattice with density  $n_\alpha = 0.22$  and a Lorentzian broadening of the spectral function  $\Gamma = 0.4t_\alpha$  uniform in  $\mathbf{k}$ -space. (b) Model  $d$ -wave pseudogap state (see text), with  $\Delta_0 = 0.1t_\alpha$ ,  $\Gamma_0 = 0.05t_\alpha$ ,  $\Gamma_1 = 0.4t_\alpha$ . The plot is for a hole-doped system ( $n_\alpha = 0.45$ ) with a nearest ( $t_\alpha$ ) and next-nearest neighbour ( $t'_\alpha$ ) hopping, with  $t'_\alpha/t_\alpha = -0.3$  (typical for cuprates, but similar effects are expected also for smaller  $|t'_\alpha/t_\alpha|$ ). (c) and (d): same as (a) and (b) in the presence of a harmonic trap ( $\omega_0 = 0.02t_\alpha$ ). The pseudogap and nodal-antinodal differentiation are clearly visible in both 2b and 2d.

Examples of numerically simulated spectra are given in Fig. 2, where a color intensity plot of the Raman rate (2) is shown for a fixed value of the frequency shift close to threshold. In (a), we consider the case of a uniformly broadened Lorentzian spectral function centered around the free dispersion relation in a two-dimensional square lattice:  $\xi_{\mathbf{k}}^0 = -2t_\alpha(\cos k_x + \cos k_y) - \mu$ . In (b) a phenomenological form [19] of the spectral function is used, which has been introduced in the context of high-temperature superconductors in order to capture the main aspects of the ARPES data in the non-SC (“normal”) state. The key feature entering this phenomenological form is a pseudo-gap with  $d$ -wave symmetry:  $\Delta_{\mathbf{k}} = \Delta_0(\cos k_x - \cos k_y)$  which vanishes along the zone diagonal (nodes) and is maximum e.g along  $(0, 0) - (\pi, 0)$  (antinode). A self-energy  $\Delta_{\mathbf{k}}^2/(\omega + \xi_{\mathbf{k}})$  is a convenient modelization of this effect. In addition, finite lifetimes effects are introduced, resulting in the form:  $A(\mathbf{k}, \omega) = -1/\pi \text{Im} [\omega - \xi_{\mathbf{k}} + i\Gamma_1 - \Delta_{\mathbf{k}}^2/((\omega + \xi_{\mathbf{k}} + i\Gamma_0))]^{-1}$ . This corresponds to a quasiparticle dispersion which is gapped out except at the nodes and to a width  $\Gamma_{\mathbf{k}} = \Gamma_1 + \Delta_{\mathbf{k}}^2\Gamma_0/[(\omega + \xi_{\mathbf{k}})^2 + \Gamma_0^2]$  which is largest (i.e a shorter lifetime) near the antinodes. This form of  $A(\mathbf{k}, \omega)$  also provides a reasonable qualitative description of re-

cent theoretical results for the two-dimensional Hubbard model [7]. The momentum space differentiation encoded in the model spectral function is clearly visible from the Raman intensity plot of Fig. 2b, with nodal regions displaying quasiparticles while antinodal ones are gapped out and short-lived. This illustrates how the Raman spectroscopy method can be used to determine the FS not only of a Fermi liquid but also of a strongly interacting system. This in contrast to the experimental techniques pioneered in [3], which apply to non-interacting systems.

Most cold atom experiments are performed within a (generally harmonic) trap. Thus, it is important to include the effect of the spatial inhomogeneities and verify that it does not spoil the predicted signatures. The simplest way of taking into account the trapping potential is to use a local density approximation, where the observed signal is the sum of the contributions of the different points  $\mathbf{R}$  of the trap. Spatial inhomogeneity enters via the fact that the local chemical potential has a different value at different spatial positions,  $\mu_{\mathbf{R}} = \mu - M\omega_0^2\mathbf{R}^2/2$ . The results are summarized in Figs. 2(c,d) for physical situations such that the value of the chemical potential at the trap center coincides with that of the homogeneous system in Figs.2(a,b). As expected, the intensity map is now a superposition of the Fermi surfaces corresponding to all the densities realized in the trap. The outer shell delimited by the extinction of the signal still gives a direct access to the FS corresponding to the highest densities at the centre of the trap. The typical signatures of exotic states remain clearly visible in the trap as well: in Fig. 2d, the nodal-antinodal differentiation is apparent in the outer shell of this plot as a faster decay of the quasiparticle intensity along the antinodal directions than along the nodal ones. A possible way of revealing the region around the Fermi surface is to measure the intensity maps for two, slightly different values of the frequency and/or the total atom number, and then take their difference: the resulting differential images for the trapped system (not shown) recover the same qualitative features of the homogeneous system shown in Fig. 2a-b.

The discussion so far has assumed that it is possible to repeat the measurement of the total rate  $R$  for many different values of  $\mathbf{q}$ . In some cases, a different scheme with a momentum-selective detection of the scattered  $\beta$  atoms may be instead favorable, quite similar to ARPES in solids. A single value of  $\mathbf{q}$  is used, and a time of flight expansion of the  $\beta$  atoms cloud is performed (after suddenly turning off the trap and the lattice potential) in order to reconstruct the momentum distribution of the atoms. As shown in Fig. 3a, the Raman resonance condition allows for a selective addressing of the different regions in  $\mathbf{k}$  by tuning the frequency  $\Omega$ . The number of Raman-scattered atoms with final momentum  $\mathbf{k}$  is proportional to the integrand  $n_F(\varepsilon_{\mathbf{k}\beta} - \Omega) A(\mathbf{k} - \mathbf{q}, \varepsilon_{\mathbf{k}\beta} - \Omega)$  of (2). Fig.3b shows that the resulting  $\mathbf{k}$ -space intensity

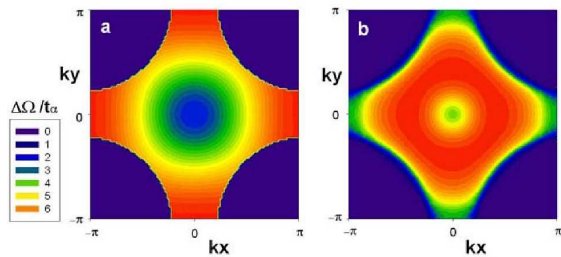


FIG. 3: (a) Colour plot illustrating the selective addressing of  $\mathbf{k}$ -space by a proper choice of  $\Omega$ . (b) Time of flight  $\mathbf{k}$ -map obtained by integrating the Raman intensity for  $\Delta\Omega$  varied in the range  $[2.4t_\alpha, 6.8t_\alpha]$ . The dispersion relation of the  $\beta$ -atoms is taken as  $\varepsilon_{\mathbf{k}\beta} = \varepsilon_\beta^0 - 2t_\beta(2 + \cos k_x + \cos k_y)$  with  $t_\beta = 1.5t_\alpha$  (note that interactions will renormalize downwards the effective  $t_\alpha$  even if bare values are equal). Parameters are as in Fig.2c and  $\mathbf{q} = 0$ .

map is able to reveal the details of the pseudogap physics, in particular its  $\mathbf{k}$ -dependence. This is an important advantage over microwave spectroscopy techniques [20] which are not momentum selective.

As a final point, we discuss some orders of magnitude which are important for the actual feasibility of the experiments proposed in this article. Specifically, we consider the example of  ${}^6\text{Li}$  atoms (see also Ref. [18]) and check that the interaction of atoms in state  $\beta$  with the Fermi gas in  $\alpha, \alpha'$  can indeed be neglected. The coupling between the two lowest states  $|\alpha\rangle = |I_z = 1, m = -1/2\rangle$ ,  $|\alpha'\rangle = |0, -1/2\rangle$  can be controlled through the Feshbach resonance at 834 G. We choose the final state to be  $|\beta\rangle = |1, 1/2\rangle$ . It has the same nuclear spin component  $I_z$  as the  $\alpha$  state and has a weak collisional cross-section  $\sigma \simeq 0.8 \times 10^{-16} \text{ m}^2$  with  $\alpha, \alpha'$  atoms [21]. Taking typical values for the lattice wavelength  $\lambda \sim 800 \text{ nm}$ , the atomic density  $\rho \sim (2/\lambda)^3$  and the recoil velocity  $v \sim h/(M\lambda)$  of atoms in state  $\beta$ , we evaluate the collision rate to be  $\gamma_c = \rho\sigma v \sim 10^2 \text{ s}^{-1}$ . The Raman detection sequence can therefore be performed in a time scale of the order of a few milliseconds, yielding an energy resolution in the 100Hz range. Losses due to inelastic transitions from state  $\beta$  have a rate  $\sim 10^{-12} \text{ cm}^3 \text{ s}^{-1}$  and can be neglected on this time scale. For the same parameters, we also checked that the mean-field interaction between an atom in  $\beta$  and the background in  $\alpha, \alpha'$  is smaller than the typical width of the atomic band in the lattice and plays only a minor role.

In summary, we have proposed a Raman spectroscopy technique which, analogously to ARPES in solid-state physics, is able to address the one-body Green's function. This technique can be used to obtain information on the Fermi surface and on the quasiparticles of a gas of fermionic atoms, even in strongly-correlated states. In the near future, this technique may play an important role in the experimental characterization of the novel quantum states of matter that can be obtained with ul-

tracold atoms in optical lattices.

We are grateful to T. Esslinger for an interesting discussion. We acknowledge support from the ANR under contract ‘‘GASCOR’’, from IFRAF, and from CNRS and Ecole Polytechnique. Laboratoire Kastler Brossel is a research unit of Ecole normale sup erieure and Universit e Paris 6, associated to CNRS.

- 
- [1] M. Greiner et al., Nature **415**, 39 (2002).
  - [2] M. Greiner et al., Nature **537**, 426 (2003); S. Jochim et al., Science **302**, 2101 (2003); M. W. Zwierlein et al., Phys. Rev. Lett. **91**, 250401 (2003); T. Bourdel et al., Phys. Rev. Lett. **93**, 050401 (2004); J. K. Chin, Nature **443**, 961 (2006).
  - [3] M. K ohl et al., Phys. Rev. Lett. **94**, 080403 (2005).
  - [4] I. Bloch, Nature Physics **1**, 24 (2005).
  - [5] A. A. Abrikosov et al., *Methods of Quantum Field Theory in Statistical Physics* (Dover, New York, 1963).
  - [6] A. Damascelli et al., Rev. Mod. Phys. **75**, 473 (2003).
  - [7] C. Honerkamp et al., Phys. Rev. B **63**, 035109 (2001); A. A. Katanin and A. P. Kampf, Phys. Rev. Lett. **93**, 106406 (2004); D. S en echal and A.-M. S. Tremblay, Phys. Rev. Lett. **92**, 126401 (2004); M. Civelli et al., Phys. Rev. Lett. **95**, 106402 (2005).
  - [8] G. D. Mahan, *Many Particle Physics* (Plenum, New York, 1981).
  - [9] D. M. Stamper-Kurn, et al., Phys. Rev. Lett. **83**, 2876 (1999); I. Carusotto, J. Phys. B: At.Mol.Opt.Phys. **39**, S211 (2006).
  - [10] S. F olling et al., Nature **434**, 481-484 (2005); M. Greiner, C. A. Regal, J. T. Stewart, and D. S. Jin, Phys. Rev. Lett. **94**, 110401 (2005); E. Altman et al., Phys. Rev. A **70**, 013603 (2004).
  - [11] A. Damascelli, Physica Scripta Volume T **109**, 61 (2004).
  - [12] E. W. Hagley et al., Science **283**, 1706 (1999).
  - [13] Y. Japha et al., Phys. Rev. Lett. **82**, 1079 (1999).
  - [14] D. L. Luxat and A. Griffin, Phys. Rev. A **65**, 043618 (2002).
  - [15] P. Blair Blakie, cond-mat/0508365.
  - [16] I. E. Mazets, G. Kurizki, N. Katz, and N. Davidson, Phys. Rev. Lett. **94** 190403 (2005).
  - [17] P. T orm a and P. Zoller, Phys. Rev. Lett. **85**, 487 (2000).
  - [18] W. Yi and L. Duan, cond-mat/0605440.
  - [19] M. R. Norman et al., Phys. Rev. B **57**, 11093 (1998).
  - [20] C. Chin et al., Science **305**, 1128 (2004).
  - [21] F. A. van Abeelen et al., Phys. Rev. A **55**, 4377 (1997).
  - [22] A. Polkovnikov, E. Altman, E. Demler, PNAS **103**, 6125 (2006).
  - [23] Q. Niu, I. Carusotto, A. B. Kuklov, Phys. Rev. A **73**, 053604 (2006).
  - [24] Information on one-particle correlators can be obtained from a measurement of two-particle ones once the system is made to interfere with either another identical system [22] or with a reference condensate [23].
  - [25] The superscript  $\dagger$  indicates that  $\psi^\dagger$  is to the left of  $\psi$  independently of the sign of  $t$ . Operators are time-evolved in the grand canonical ensemble [8].
  - [26] The accessible range of  $\mathbf{q}$  is  $0 \leq c|\mathbf{q}|/2 \leq \omega_1 \simeq \omega_2$ . In a red-detuned lattice with respect to  $\omega_{1,2}$ , all values of  $\mathbf{q}$

in the first Brillouin zone are therefore accessible.